Accepted Manuscript

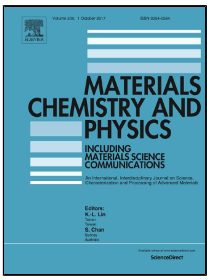

Organosilane modified bioactive glass/poly (amido amine) generation 5 hybrids: effect of solvent and synthesis route on structural properties, thermal stability and apatite formation

Fakhraddin Akbari Dourbasha, Parvin Alizadeh

PII:	S0254-0584(17)30726-5
DOI:	10.1016/j.matchemphys.2017.09.023
Reference:	MAC 19990
To appear in:	*Materials Chemistry and Physics*
Received Date:	05 April 2017
Revised Date:	14 June 2017
Accepted Date:	13 September 2017

Please cite this article as: Fakhraddin Akbari Dourbasha, Parvin Alizadeh, Organosilane modified bioactive glass/poly (amido amine) generation 5 hybrids: effect of solvent and synthesis route on structural properties, thermal stability and apatite formation, *Materials Chemistry and Physics* (2017), doi: 10.1016/j.matchemphys.2017.09.023

Highlights

Hybrids of silica bioactive glass and poly (amido amine) dendrimers are synthesized.

Hybridization improves thermal stability and biomineralization activity of hybrids.

Structure-property relationship, derived from solvent and procedure, is discussed.

The very hybrid can be used for further studies in bone regeneration.

Organosilane modified bioactive glass/poly (amido amine) generation 5 hybrids: effect of solvent and synthesis route on structural properties, thermal stability and apatite formation

Fakhraddin Akbari Dourbash [a]; Parvin Alizadeh [a*]

[a] Department of Materials Science & Engineering, Faculty of Engineering & Technology, Tarbiat Modares University, P. O. Box: 14115-143, Tehran, Iran

*Corresponding Author: Professor Parvin Alizadeh,

Corresponding Author's Institution: Tarbiat Modares University

Corresponding Author's Email: P-Alizadeh@modares.ac.ir

Corresponding Author's phone: +98 21 82884399

Abstract

For hybrid materials, molecular interactions between inorganic and organic phases which are dependent upon the solvent and the procedure through which a hybrid is synthesized, directly affect the macroscopic properties. We report herein the effect of solvent (dimethylformamide (DMF) and dimethyl sulfoxide (DMSO)) and synthesis route (freeze drying or heat treatment) on structural and microstructural properties, thermal stability and the apatite forming ability of silica/poly (amido amine) generation 5 (PAMAM G5) class II hybrids. Thorough investigations of the hybrids allowed us to prove the covalent coupling between inorganic and organic chains and inorganic condensation, as well as the nanoscale interactions and co-network of inorganic and organic phases. Furthermore, thermal stability and silica network dissolution were studied and a clear conclusion was drawn as to improved thermal stability and a steady degradation is achieved by incorporation of silica phase and a coupling agent. The biomineralization capability of hybrids was evaluated by immersing in simulated body fluid (SBF) for 1 week. SEM, ICP-OES, FTIR and XRD showed that hybrids synthesized by both DMF and DMSO could form, although with different morphologies, an apatite layer on their surface and therefore are highly bioactive. Our results suggest that silica/PAMAM G5 hybrids could further have promising applications in bone tissue engineering.

1. Introduction

Hard and soft tissue engineering employs strategies and materials to encourage body's natural repair systems [1]. Depending on the application and the method, from seeding cells on the scaffold *in vitro* to seeding stem cells taken from bone marrow on scaffolds prior to implantation, there are many criteria, either for the materials used or the techniques applied, that must be

fulfilled in order to have a successful tissue regeneration [2]. Biocompatibility, the ability to not produce an adverse immune response, bioactivity, the ability to bond to the existing bone, biodegradability, the ability to degrade at a rate compatible to tissue formation without toxic degradation products, and good mechanical properties are amongst the important criteria for a material to be used in a tissue regeneration strategy [3, 4]. Bioactive glasses are bioactive, degradable and have compressive strength similar to porous bone and therefore meet the requirements for a bone graft material, however they suffer brittle failure under cyclic loading [5, 6].

Composite and nanocomposite materials seem to be a promising solution in overcoming the problems associated with single organic or inorganic phases [7]. However, in composites macroscale phase domains would result in unpredictable dissolution rate and rapid loss of mechanical properties [8]. In addition, synthesizing monodisperse and homogenous nanocomposites would be difficult [9]. Class II inorganic-organic hybrids in which a polymer is functionalized with an organosilane and then covalently bonded to an inorganic phase is an alternative to composites and nanocomposites [10, 11]. Recently, by acquiring sol-gel method, various polymers such as, poly (vinyl alcohol) [12, 13], gelatin [14], chitosan [15], poly (γ-glutamic acid) [16], poly (methyl methacrylate) and poly (ε-caprolactone) [17] were covalently bonded to inorganic silica phase by silane coupling agents and formed class II hybrids.

Surface-to-volume ratio and interfacial area between the two phases are known to directly affect the dissolution rate and physicochemical properties of a hybrid material and since sol–gel is a versatile low-temperature technique and materials synthesized by this approach have high surface-to-volume ratio, sol-gel has long been adopted to synthesize hybrids [18-21]. Solvents stabilize the steric forces and allow dispersion of the two phases, therefore molecular interactions in the sol are directly affected by the nature of solvent [22, 23]. Moreover, bonding between the phases that ranges from non-covalent attractive forces such as hydrophobic interactions, hydrogen bonding, and ionic interactions (class I hybrid) to covalent coupling through an organosilanes (class II hybrid) is of utmost importance in determining the hybrids properties [7]. In addition, there are some requirements for the organic phase to be met so that a successful inorganic-organic hybrid could be synthesized. Synthetic biocompatible polymers having nucleophilic functional groups such as -NH_2, -OH and -COOH capable to be functionalized by an organosilane are favorable for hybrid synthesis [8]. Also, polymer must be incorporated into the sol, which requires the polymer to be soluble in the silica precursor, water, and also sol-gel by-product, alcohol [11]. Poly (amido amine) generation 5, PAMAM G5, polymers are biocompatible, nonimmunogenic, water-soluble, and possess terminal modifiable amine functional groups that can be functionalized by 3-glycidoxypropyltrimethoxysilane (GPTMS) [24].

To this end, we have chosen PAMAM G5 polymers to synthesize class II hybrids through direct hybridization by GPTMS which contains an organic functionality to bond to PAMAM and three methoxysilane groups which hydrolyze and undergo condensation with the inorganic phase.

Also, the homogeneity of the polymer hybrids is strongly dependent on the type of solvents, and, DMF and DMSO are strong polar solvents and may increase chain stretching of the polymer and therefore cross-linking density. Also, since the production of a free-standing monolith with 60% inorganic phase is the aim of this study, and DMF and DMSO are proved to be successful in this regard [25], we have chosen to synthesize hybrids in DMF and DMSO. The hypothesis was that the covalent coupling between NH_2 functional groups of PAMAM dendrimers and epoxy ring of GPTMS, along with condensation of Si-OH groups to Si-O-Si bonds, would result in an interpenetrating organic/inorganic network with enhanced physicochemical properties. Finally, the effect of solvent and synthesis route on thermal stability, physicochemical properties and apatite formation is studied. We hope this investigation would provide new insights on important parameters which define the final properties of PAMAM/silica hybrids. Overall, the results would be further useful in fabricating a hybrid material for bone regeneration.

2. Experimental

2.1. Materials

Tetraethylorthosilicate (TEOS, 99.0%), 3- Glycidoxypropyltrimethoxysilane (GPTMS, 97.0%), ethylenediamine (EDA), dimethyl sulfoxide (DMSO), methyl acrylate (MA), calcium chloride ($CaCl_2$), methanol and hydrochloric acid solution (1M HCl) were all purchased from Merck Co. and were used without further purification.

PAMAM dendrimers were synthesized following a two-step process, involving Michael addition of a suitable amine initiator core with methyl acrylate (MA), and exhaustive amidation of the resulting esters with large excess of ethylenediamine (EDA); a strategy known as the divergent synthesis method [26].

2.2. Preparation of Silica/PAMAM hybrids

2.2.1. Hybrids synthesized by freeze drying approach: PAMAM/silica hybrids were synthesized using the one-pot reaction procedure described as below. Briefly, 10 mg of PAMAM was dissolved in 10 ml deionized water. 2N hydrochloric acid (HCl) was added dropwise to adjust the pH of the solution to 4 for further functionalization with GPTMS. Higher pH can accelerate gelation due to the condensation of end silanol groups of the GPTMS molecule, while lower pH can catalyze epoxide ring opening, resulting in hydrolysis of epoxide ring to the corresponding diol being the prevailing reaction and therefore removing the potential nucleophilic attack sites [27, 28]. Thus, the pH of 4 was chosen to give the reaction the best time course between condensation of the silicate network, epoxide ring opening and the subsequent nucleophilic attack. Then, appropriate amount of GPTMS was added to the PAMAM G5 solution so that the molar ratio of 1:128 was obtained. Here, it was assumed that each of 128 PAMAM amino groups (NH_2) force-open the epoxy group of GPTMS to form a NH-O bond.

After stirring at room temperature for 48 h, the resultant PAMAM-GPTMS precursor solution was frozen in liquid nitrogen (-175 ℃). The frozen hybrids were subsequently transferred to a freeze-dryer (SUBLIMATOR, VaCo5, ZIRBUS technology, Germany) and the samples were lyophilized for 12 h to complete dryness. The hybrids are called SiPAm (FD), where Si stands for **Si**lica, PAm stands for **P**oly (**Am**ido **Am**ine) and FD stand for **F**reeze **D**ried.

2.2.2. Hybrids synthesized via sol-gel technique and through aging and drying: The PAMAM solution with a concentration of 10 wt% was prepared by dissolving PAMAM G5 in DMF (DMSO) under stirring at 60 ℃. Then, certain amount of GPTMS dissolved in DMF (DMSO) was added drop-wise to the PAMAM/DMF (DMSO) solution and allowed to react for 12 h under a constant flow of N_2 while stirring. Additionally, a silicate bioactive glass sol with Si/Ca mol ratio of 70/30 was prepared by mixing tetraethylorthosilicate (TEOS), hydrochloric acid and calcium chloride under vigorous stirring. The silicate bioactive glass sol was added to the PAMAM/GPTMS solution. After stirring for 1 h, hydrofluoric acid (HF) was added to catalyze the inorganic condensation. Then, the hybrid sol was immediately sealed and transferred to a heated oven. The sealed samples were aged at 60 ℃ for 4 days followed by opening the molds to dry at 60 ℃ for 6 days until complete dry. The samples synthesized in DMF and DMSO are called SiPAm (DMF) and SiPAm (DMSO), respectively. The synthesis route designed for crosslinking PAMAM with GPTMS and condensation of inorganic species to form PAMAM/silica hybrids is schemed in Fig. 1.

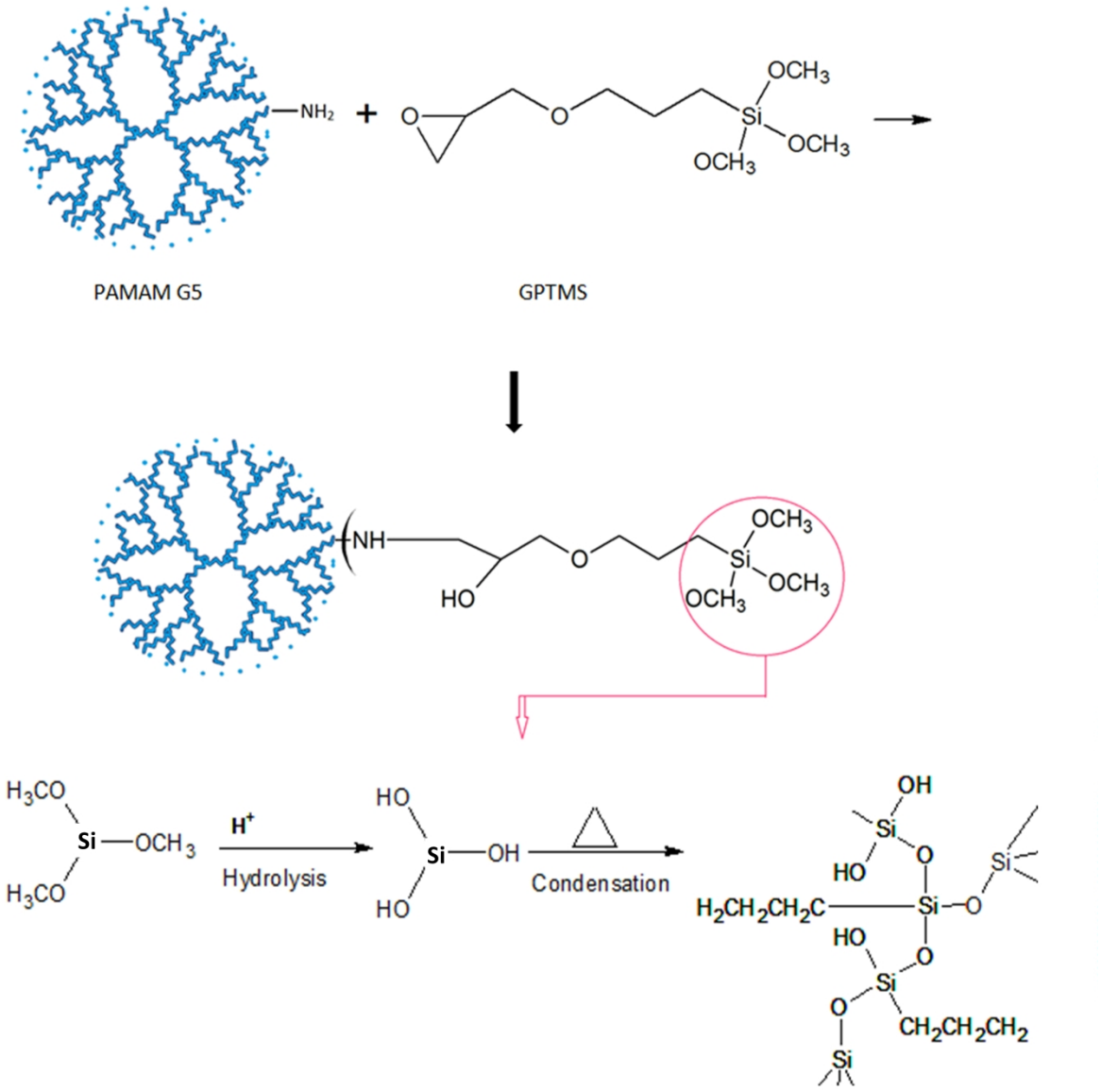

Fig. 1. Chemical structure and reaction model for cross-linking PAMAM to prepare PAMAM/silica hybrid.

2.3. Characterization methods

2.3.1. Chemical structure characterization

Fourier Transform Infrared spectroscopy (FTIR) was performed on a PerkinElmer Frontier FTIR spectrometer in the range of 400–4000 cm^{-1}. All samples were mixed with

dry KBr, ground down to fine powders and pressed into pellets. Spectra were obtained in room temperature and were taken as the average of 32 scans at a resolution of 4 cm^{-1}.

2.3.2. Morphological and microstructural characterization

Porous network of the hybrids was determined using Nitrogen adsorption (PMI N_2-BET Sorptometer (Porous Materials, Inc. NY, USA)). 100 mg of samples were degassed at 120 °C for 8 h before analysis. The apparent BET surface area was calculated by fitting nitrogen adsorption data to the BET equation. The Barrett-Joyner-Halenda (BJH) method was also applied in order to determine the pore size distribution.

The surface and particle morphology was characterized using Field Emission Scanning Electron Microscopy (FESEM, TESCAN-MIRA 3 LMU) at an accelerating voltage of 20 kv and by mounting the samples on double sided carbon tape and sputter-coating with a thin layer of gold before observation. Transmission Electron Microscopy (TEM, Philips CM 30) at an accelerating voltage of 200 kv was used to study the powder samples deposited on holey carbon TEM grids.

2.3.3. Thermal stability test

Thermal properties of hybrids were evaluated by a Mettler Toledo TGA/SDTA851 analyzer in a nitrogen atmosphere. The hybrids with a typical sample weight of 6 mg were placed in a platinum crucible and heated from room temperature up to 900 ℃ at 10 ℃ min^{-1}.

2.3.4. *In vitro* biodegradation study

The *in vitro* bioactivity of hybrids was evaluated by examining an apatite formation on their surfaces in simulated body fluid (SBF) solution. The SBF solution has a similar chemical composition to blood plasma. The samples with a concentration of 1.5 $mg.ml^{-1}$ were maintained in SBF at 37 ℃ and were agitated at constant rotation speed of 120 rpm for 1 week and then removed from the fluid and immersed in DI water overnight to remove any soluble inorganic ions. After air-drying in room temperature for 2 days, the *in vitro* apatite forming bioactivity was also tested by scanning electron microscopy (SEM, Phenom-FX25) with energy dispersed spectroscopy (EDS) and FTIR spectra (FTIR, PerkinElmer Frontier). The Ca, Si and P ion concentrations in the filtered solutions were also quantified by inductively coupled plasma optical emission spectroscopy (ICP-OES, Varian 730-ES, USA). After 1, 8, 24, 72 and 168 h, 1 ml of solution was removed and filtered. To compensate for the removed solution, 1 ml of fresh SBF was added to the original test solution.

3. Results and discussion

3.1. FTIR study of hybrids

FTIR spectra of the PAMAM G5 dendrimer, GPTMS and the PAMAM/silica hybrids within the range of 400 to 4000 cm^{-1} are shown in Fig. 2. N-H stretching vibration of primary amine and amide groups are observed at 3534 cm^{-1} and 3382 cm^{-1}, respectively. The peaks at 1711 cm^{-1} and

1625 cm^{-1} are characteristic C=O stretching and N-H bending vibration of amide group in the periphery of PAMAM. Also, the appearance of peaks at 2934 cm^{-1} and 2972 cm^{-1} are due to the C-H stretching and the peaks at 1342 cm^{-1} and 1046 cm^{-1} are attributed to the stretching vibration of C-N and C-O groups, respectively.

In the FTIR spectrum of GPTMS the bands from 2841 to 2943 cm^{-1} were assigned to symmetric and asymmetric stretching of C-H bond in glycidoxypropyl part of the GPTMS. The absorption peak which appeared at 1254 cm^{-1} confirms the presence of Si-OCH_3 linkage in GPTMS. Also the peak at 909 cm^{-1} is due to the epoxy ring.

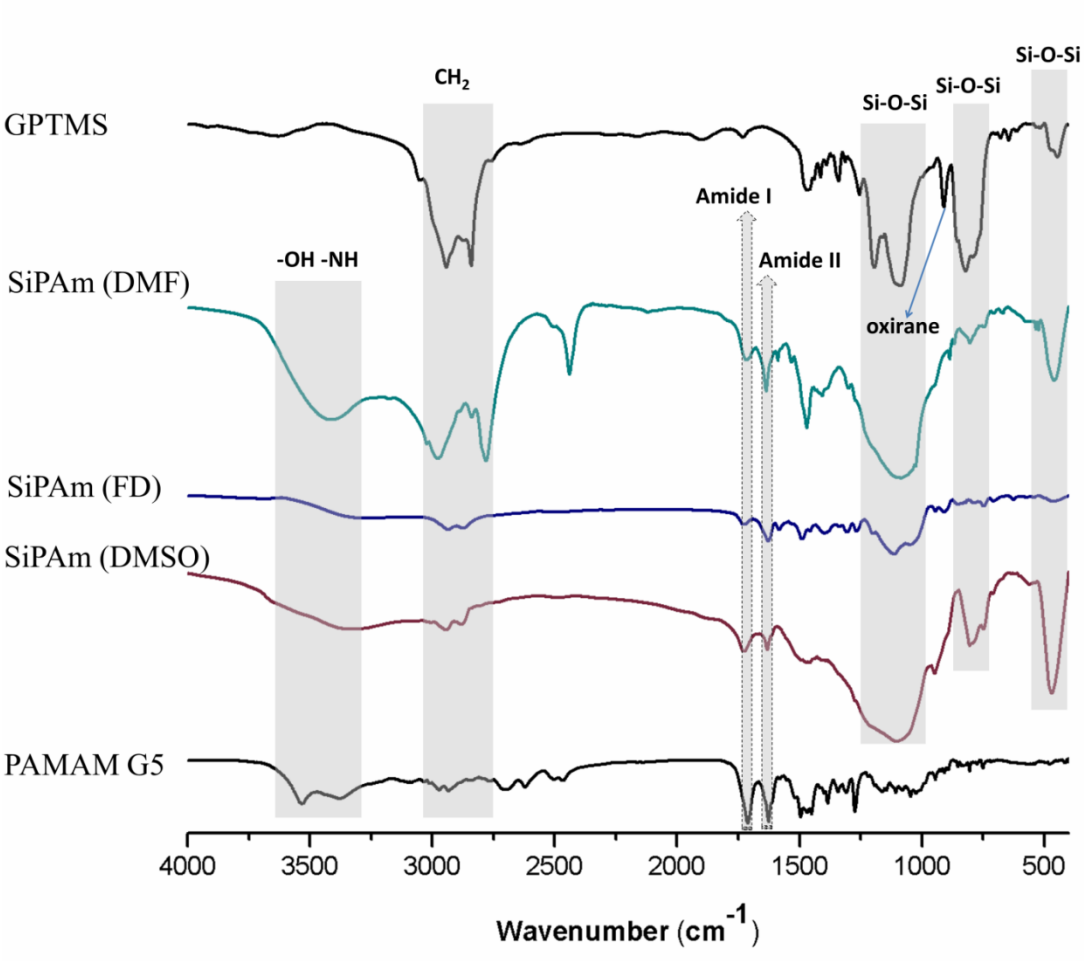

Fig. 2. FTIR spectra of PAMAM, GPTMS and the synthesized hybrids.

As can be seen in Fig. 2 the absorption bands around 820 cm^{-1} in GPTMS, due to Si-O (CH_3) symmetric stretching vibration and around 909 cm^{-1} due to the oxirane ring, are vanished, indicating epoxy ring opening and inorganic hydrolysis. Furthermore, hydrolysis is confirmed by the change in the GTPMS absorption bands at 2943 and 2841 cm^{-1} which are attributed to C-H

asymmetric and symmetric stretching in Si-O-CH_3, respectively [29]. Compared with FTIR spectrum of GPTMS and PAMAM, new absorption bands at around 1115,749 and 464 cm^{-1} were observed in FTIR spectra of all the silica/PAMAM hybrids. They could be assigned to Si–O-Si vibrations [27, 30]. With introducing silane groups into the polymer, the infrared spectra showed absorption at 907 cm^{-1} which is associated with the stretching of Si-OH bonds. The reaction between amine groups in PAMAM and oxirane groups in GPTMS was observed with the intensity decrease of the absorption band at 1625 cm^{-1} (N-H bending of the primary amine) and the shift of Amide I bands to higher wavenumbers [31].

3.2. Characterization of structure and morphology

The morphology and microstructure of hybrids are shown in Fig. 3 and Fig. 5. First of all it must be stated that the hybrid samples with DMSO and DMF and synthesized through sol-gel technique and by aging and drying were free-standing monoliths, while the samples synthesized by freeze drying did not form any shape and turned to be in the form of powders.

All the samples were composed of fused silica nanoparticles characteristic of sol-gel. However, the morphology and the size of the nanoparticles were different in all three hybrids.

SiPAm (DMF) and SiPAm (DMSO) showed relatively smooth fracture surface, as can be seen in Fig. 3A and Fig. 5A. High magnification SEM image shown in Fig. 3C which is the zoom-in image of the surface morphologies of SiPAm (DMF) samples also proved their dense structure with nanoscale distributions and showed that the samples were composed of interpenetrating continuous networks of silica nanoparticles embedded in a polymeric matrix. However, secondary SEM images presented in Fig. 3D, along with EDS analysis which are indicative of wt% and at% of yellow squares (C and D) showed that phase separation of the inorganic phase in the polymer matrix may have occurred in SiPAm (DMF) hybrids and might be due to the poor interactions between Ca and the polymer chain. In addition, this phase separation may be explained from the crosslinking points and lower cross-linked density and molecular interactions in hybrid as DMSO possesses a high polarity than DMF. Therefore PAMAM polymers would have high solubility and chain stretching in DMSO and the result would be an increase in bonding intensity between inorganic and organic species and therefore homogeneity of the micro and nanostructure. The ultrastructural image of the sol–gel processed hybrids demonstrated that the samples were organized on the nanoscale, with silica nanoparticulares being embedded within the PAMAM matrix. Moreover, a homogeneous morphology was observed at the micro-scale. This suggests that the sol–gel process is effective in achieving a level of organization that allows the two components to be hybridized so as to elicit synergistic effects.

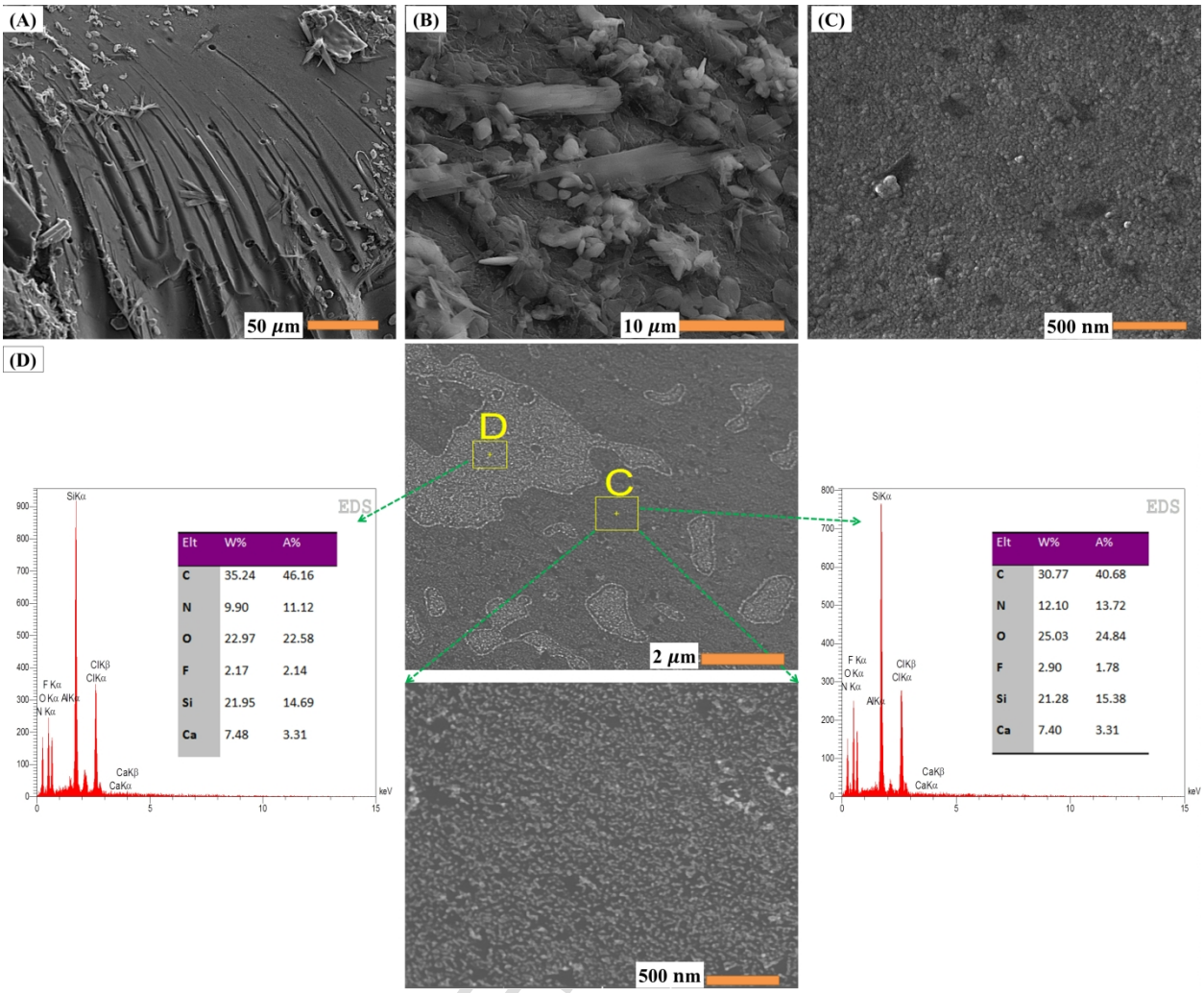

Fig. 3. Surface morphology (A and B), microstructure (C and D) and corresponding EDS analysis of marked areas of SiPAm (DMF) hybrids.

Furthermore, SiPAm (DMF) hybrid monoliths' UV-vis spectrum shown in Fig. 4 indicated a rather low transmittance in the visible region which might be due to the phase separation and the aggregation of silica nanoparticles which form larger particles. According to the Rayleigh equation, the silica particle with a larger size (>50 nm) results in serious light scattering, therefore decreasing the transmittance [32].

As shown in Fig. 5C and D, the nanoparticles morphology in SiPAm (FD) was different than that of other hybrids. Here, silica nanoparticles seemed to be separate rather than fused nanoparticles derived from heat treatment in sol-gel process.

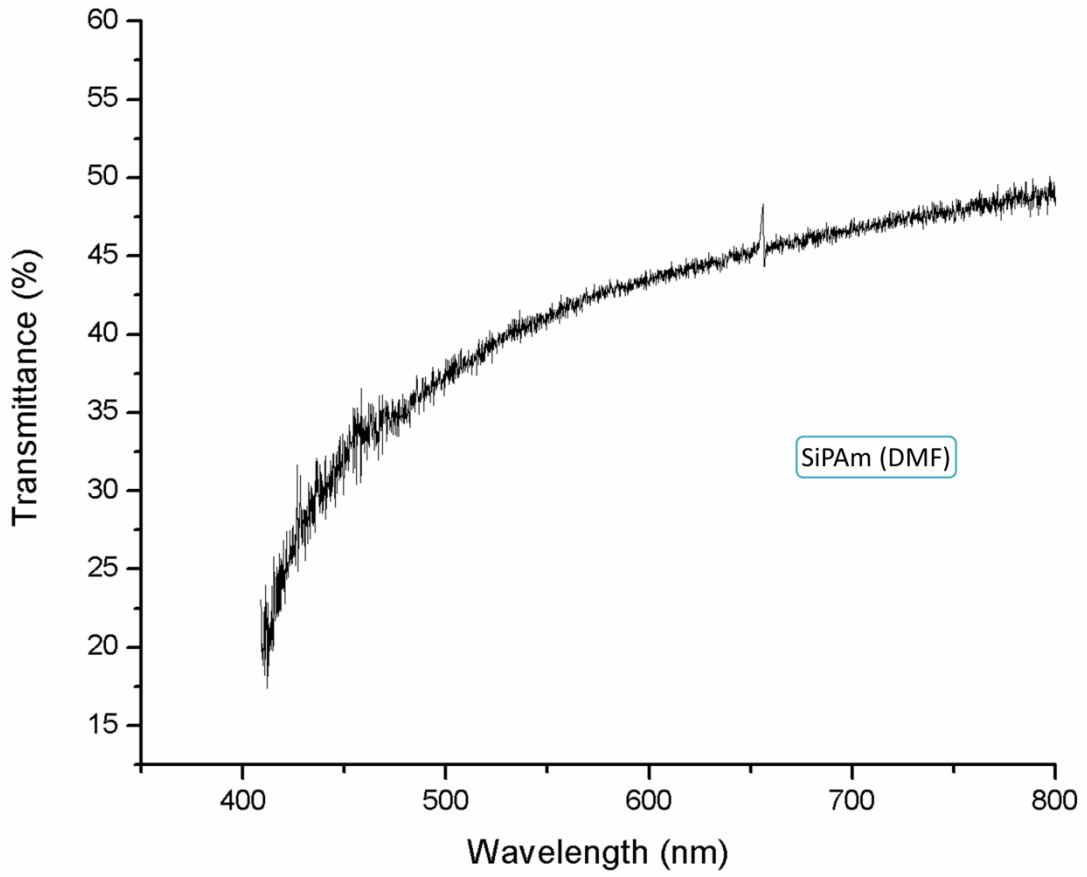

Fig. 4. UV-vis absorption spectra of the SiPAm (DMF) hybrids.

The morphology of nanoparticles also differed from the heat treated hybrids as it has been proven that amine-terminated dendrimers may act as template in the formation of silica nanospheres [33], and it is hypothesized that during hybrids synthesis, the silica network forms first by polycondensation while PAMAM dendrimers act as a template or surfactant and influence the formation of silica network, however as the freeze drying process does not include any heat treatment stage the nanoparticles are separate rod-like particles rather than fused ones. The presence of the silica phase and the calcium phase in the hybrids was confirmed by EDS analyses, shown in Fig. 3.

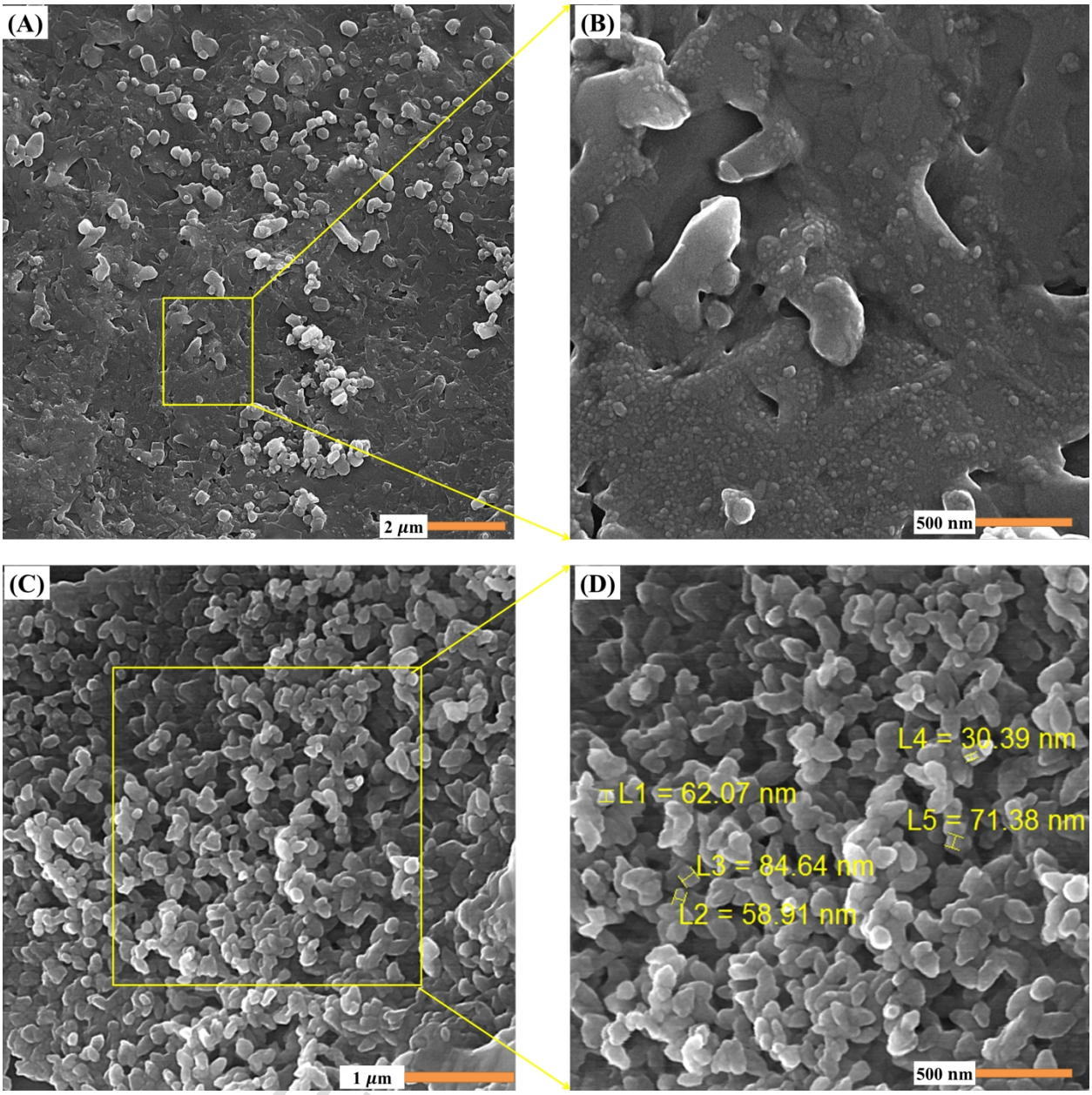

Fig. 5. Morphology and microstructure of SiPAm (DMSO) (A and B), and, SiPAm (FD) (C and D) hybrids.

Furthermore, L. Russo et al [34] worked on bis (3-amino propyl) polyethylene glycol/silica hybrids and concluded that the reaction between the amine groups of dPEG and epoxy rings of GPTMS was delayed until drying stage since -NH_2 functional groups were unavailable for nucleophilic attack, as they were involved in the catalysis of silica network formation. This suggests that because of the absence of aging and drying in freeze dried samples, silica network was formed first and most of the amine groups were unreacted as proven by FTIR analysis.

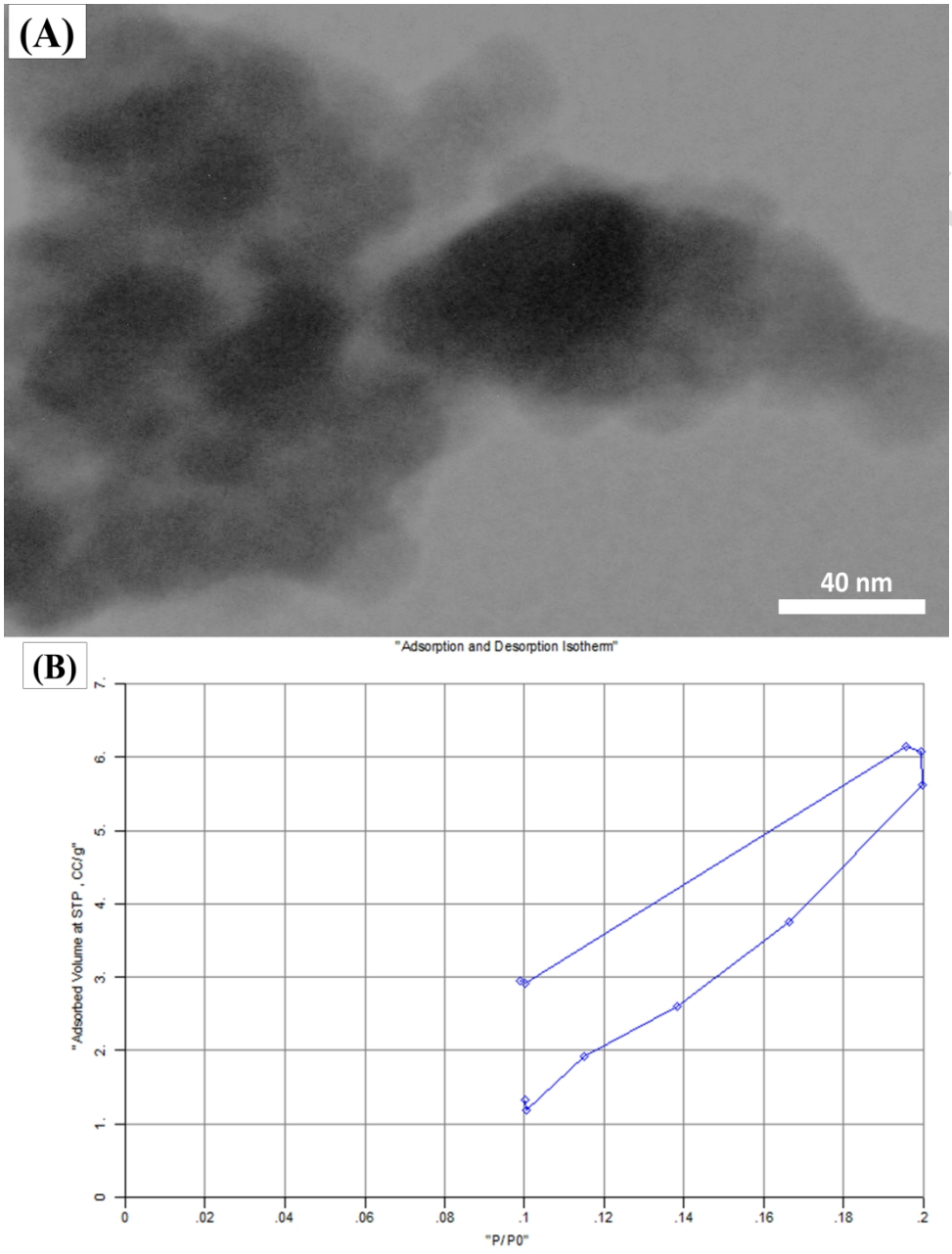

Fig. 6. TEM image (A) and N_2 sorption (B) isotherm of the SiPAm (DMF) hybrids.

In the TEM micrographs, the difference in the electronic transmission between organic and inorganic phases helps to assign the dark area to silica particles, covalently bonded to the organic matrix. As seen in Fig. 6 (A) the curved edges and waves of dark and light contrast seen in TEM image of SiPAm (DMF), were indicative of particles of higher atomic mass (silica) embedded in a lower atomic mass material (PAMAM) and it revealed that an interconnected network of silica nanoparticles were formed throughout the hybrid. Fig. 6 (B) also shows that a negligible amount

of nitrogen was adsorbed, therefore it can be concluded that a small amount of mesopores were present in the SiPAm (DMF). This supports the notion that the polymer was filling the mesopores in a continuous silica network within the hybrid.

3.3. Thermal stability of hybrids

The decomposition profiles of PAMAM, SiPAm (FD) and SiPAm (DMF) hybrids were evaluated by TGA analysis in a temperature range from 20 ℃ to 900 ℃ (Fig. 7). The first decomposition step for pure PAMAM started from 100 ℃ and is related to the water evaporation. The gradual weight loss of 5% continues until 200 ℃, while the second rapid weight loss was observed in the 200–490 ℃ temperature range and was attributed to the decomposition of PAMAM main chains.

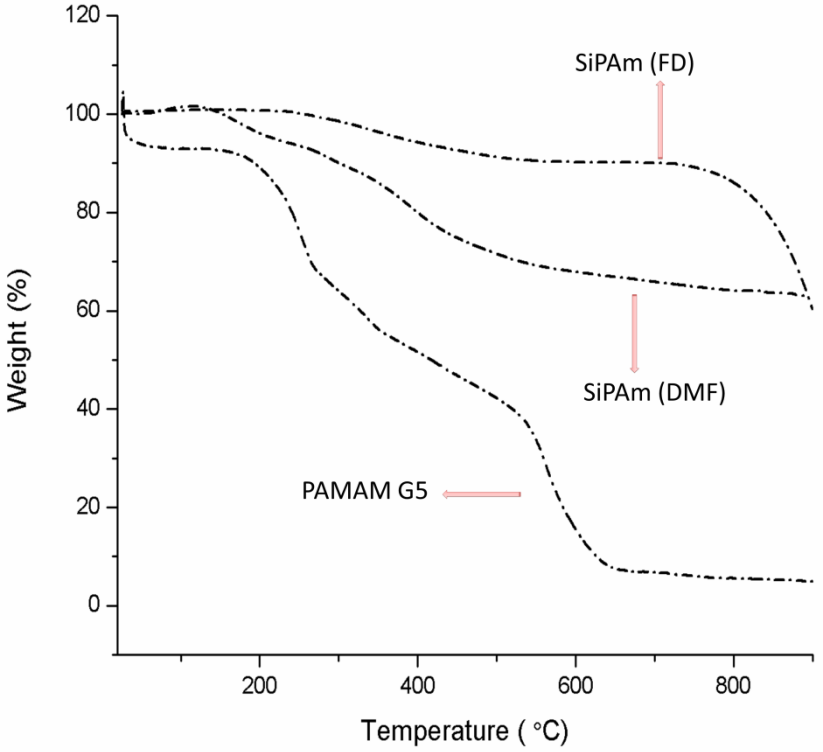

Fig. 7. TGA thermograms of PAMAM G5, SiPAm (DMF) and SiPAm (FD) obtained under nitrogen atmosphere.

In case of hybrids, the gradual weight loss of up to 5% shifted from 100 ℃ to approximately 200 ℃ for SiPAm (DMF) and even to higher temperatures (300 ℃) for SiPAm (FD). The second stage of the TGA curves is associated with the decomposition of the organic phase. The onset temperature of organic phase decomposition shifted to higher temperatures and continued to 320 ℃ for SiPAm (DMF) and 400 ℃ for SiPAm (FD). It seems that freeze dried samples exhibited better thermal stability than hybrids synthesized with aging and drying steps. It is also worth

noting that there was no initial weight loss in PAMAM/silica hybrids (specially for freeze dried samples) related to water evaporation which indicates that the condensation of silanol groups was practically complete [35]. In addition, no observed weight loss with PAMAM/silica hybrid samples might indicate that these hybrids contained no water or less water than pure PAMAM. This result implied that the degree of swelling of PAMAM/silica should be lower than that of pure PAMAM [31]. A fixed (silica cross-linked) and a swollen (PAMAM chains) domain might form in the hybrids to ensure their application for biodegradable materials and drug releasing system. The 4 % residual for pure PAMAM might be attributed to carbon-related products formed at high temperature. These results demonstrated that silica phase incorporation significantly enhanced thermal stability of hybrids.

3.4. Biomineralization on the hybrids

Shown in Fig. 8 are representative SEM images and the corresponding EDX spectrum of hybrids synthesized by DMF and DMSO and mineralized in SBF at 37 ℃ for 1 week. Low magnification image of the surface of SiPAm (DMSO) after 7 days shows that mineral phase deposited is agglomerates of spheroid crystals and high magnification SEM image (Fig. 8 (C), inset) shows that these random spherical-shaped clusters are aggregates of needle-like apatite crystals. However, apatite crystals mineralized on the surface of SiPAm (DMF) exhibited a plate-like morphology (Fig. 8 (A) and (B)).This result is rather interesting and needs further investigation as HAP crystals in vertebrate long bones and tooth enamel have a plate-like morphology [36]. EDS spectra of the hybrid monoliths show the peaks of calcium (Ca) and phosphorous (P) that, unlike O, C and N which stem from both PAMAM and the deposited mineral, can only be due to the deposited mineral which is apatite crystals.

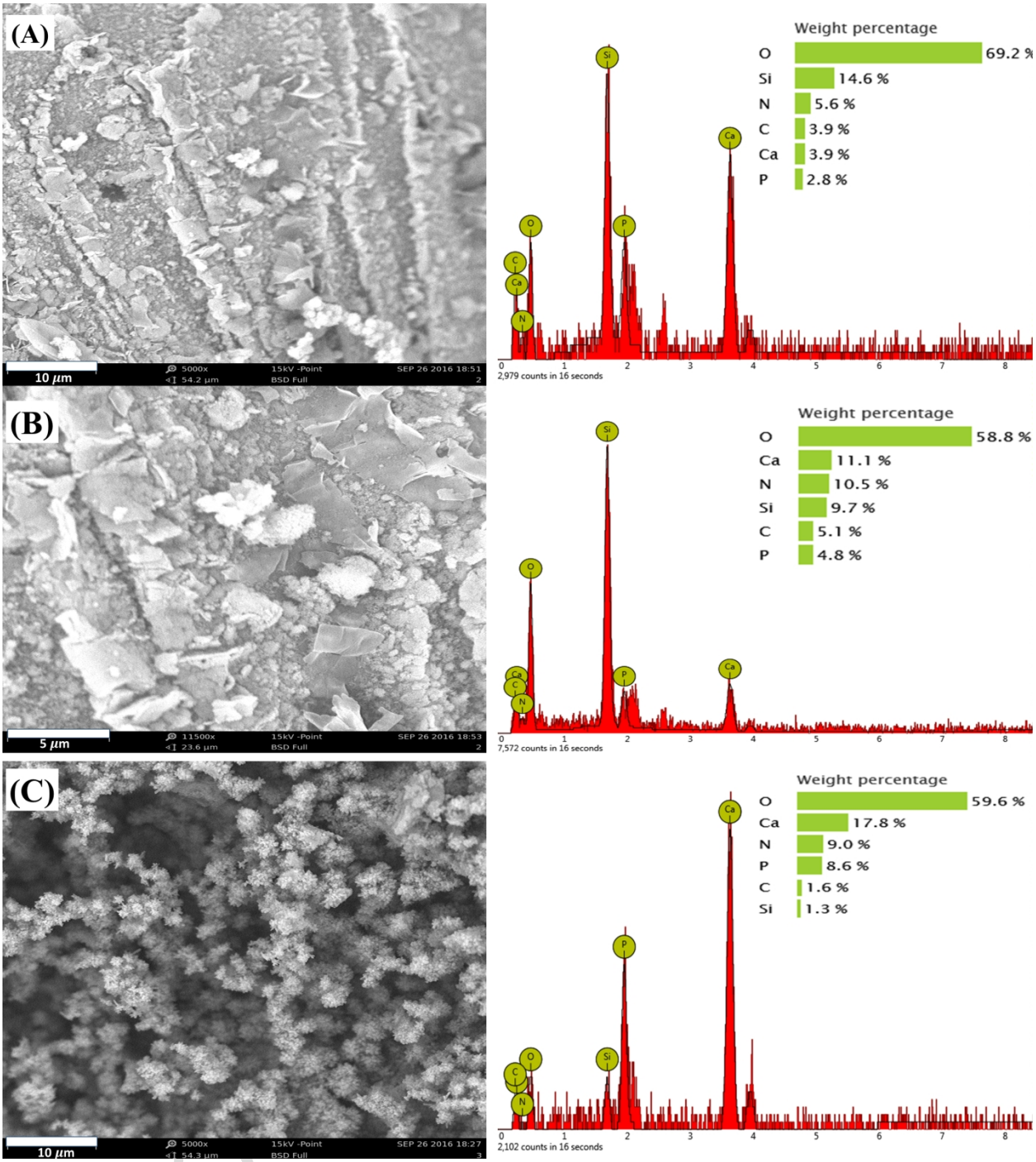

Fig. 8. SEM image and corresponding EDS analysis of the apatite formed on the surface of SiPAm (DMF) (A and B) and SiPAm (DMSO).

Moreover, Fig. 9 shows the Si, Ca and P ions released from the SiPAm (DMF) and SiPAm (DMSO) as a function of soaking time. The silicon release profile in both samples followed a similar trend and the silicon content in solution increased by increasing soaking time. However,

the amount of silicon released to the solution for SiPAm (DMF) hybrids was higher that SiPAm (DMSO), indicating that the silica network dissolution in samples synthesized by DMSO was slower than those synthesized by DMF. This difference in dissolution rate may be explained by the amount of Si-O-Si bonds (bridging oxygen) and covalent cross-linking between inorganic silica and organic polymer being greater in the samples synthesized in DMSO due to higher polarity of DMSO rather than DMF and therefore increased bonding density. In addition, a gradually decrease in Ca and P concentration was observed for both samples over the period of 1 week. The decrease in both Ca and P concentrations can be attributed to the consumption of these ions for the formation of the apatite layer.

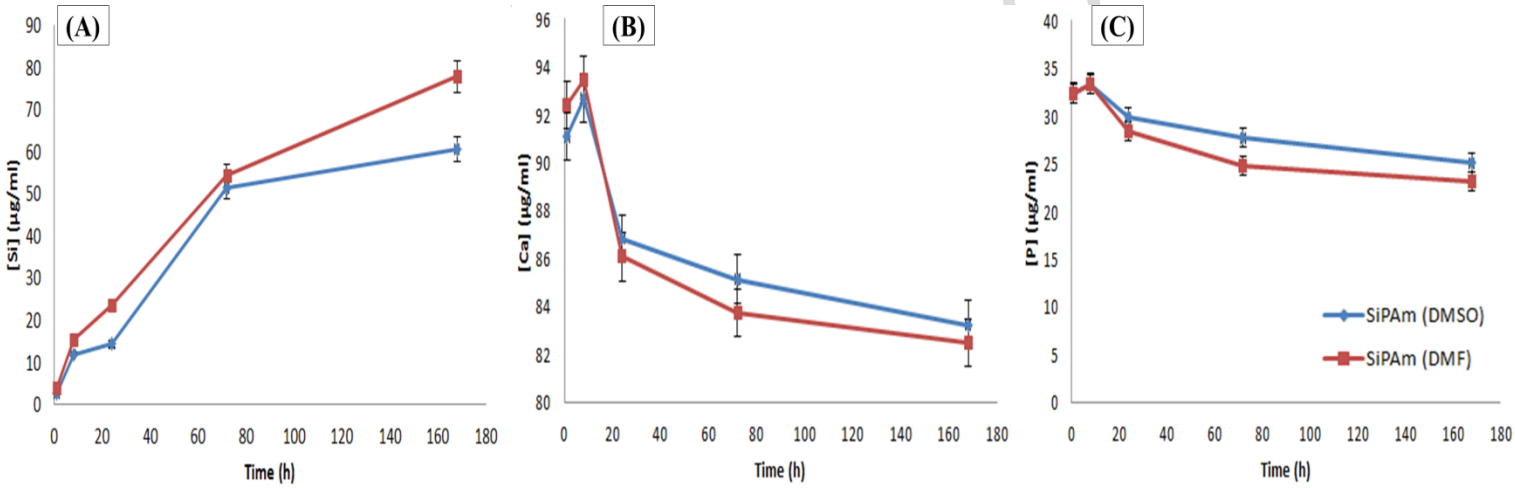

Fig. 9. Si (A) Ca (B) and P (C) ions release profiles of hybrids soaked in SBF for up to 1 week, measured by ICP-OES analysis.

To get further insight into the apatite layer formed on the hybrids the FTIR spectra were examined (Fig. 10). By day 7, hybrids exhibited characteristic phosphate and carbonate bands which confirm the formation of apatite layer. The absorption bands of the phosphate (PO_4^{3-}) groups are found between 1030-1200 cm^{-1} (asymmetric P–O stretching mode, υ_3) and at around 604 and 567 cm^{-1} (O–P–O bending mode, υ_4). The characteristic band corresponding to the carbonate (CO_3^{2-}) groups is detected around 1400-1500 cm^{-1} (asymmetric stretching mode, υ_3) for both samples.

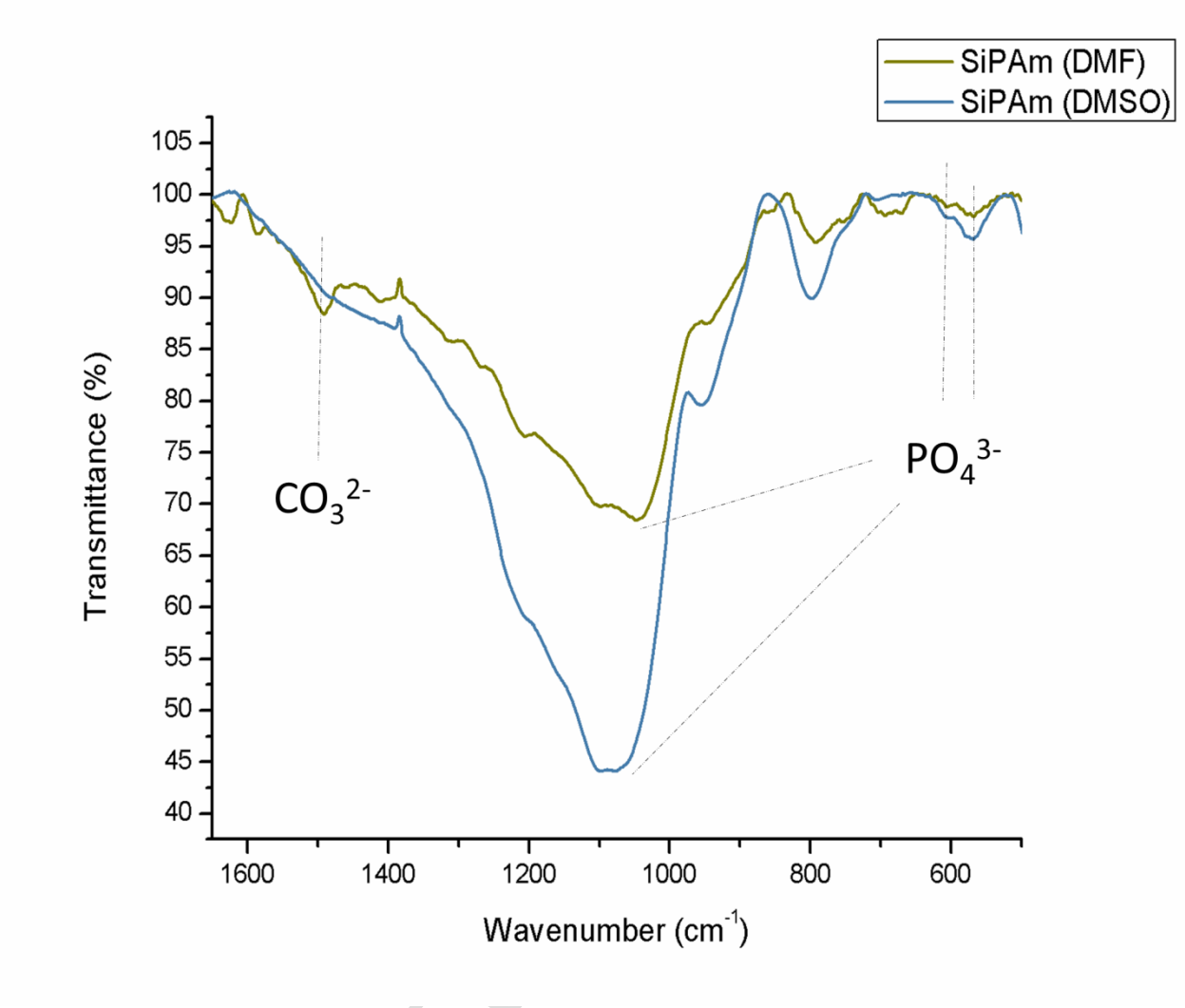

Fig. 10. FTIR spectra of minerals formed on the hybrids surface after 7 days of mineralization in SBF.

It is also worth mentioning that the hybrids synthesized with DMF could not preserve their shape after 7 days of soaking in SBF. In general, when an inorganic phase is poorly distributed within an organic phase, the inorganic particles often serve as the point of origin of failure, which decreases the strength of the hybrid and resulted in more silicon release which represents the material loss. The gradual release of the ions from the hybrids is required to form bone like apatite. Although faster release of the ions may accelerate the formation of apatite, since silicon ions form silanol groups act as nucleation sites and calcium and phosphorous ions lead to the supersaturation of the SBF solution around the hybrids, but faster release of silicon ions that are the backbone of the hybrids may result in the decrease of strength which is the case in here for DMF synthesized hybrids. Therefore, it may be necessary to control the degradation properties

based on the required application which is obtainable by changing the degree of crosslinking agent [37].

Overall, these findings provide evidence for the formation of an apatite layer on the surface of the hybrids with different morphologies for hybrids synthesized by DMF or DMSO.

4. Conclusions

Bioactive silica glass/poly (amido amine) generation 5 class II hybrids are synthesized using DMSO and DMF solvents and by two distinct synthesis procedures which are heat treatment and freeze drying. We demonstrated that hybridization per se endows hybrids with higher thermal stability. However, compared to DMF-synthesized samples, much better thermal resistance and homogeneity of microstructure were observed for hybrids synthesized in DMSO, while freeze dried samples showed much more thermal stability than both heat treated samples. BET analysis showed that hybrids had a microporous structure and TEM proved the formation of co-networks of inorganic and organic phases throughout the hybrids. Furthermore, evaluating degradation of hybrids by monitoring Si ion release to the SBF via ICP-OES proved the steady release of silicon ions. Moreover, apatite nucleation and growth occurred on the surface of hybrids after 1 week of immersion in SBF and the morphology of mineralized layer was dependent upon the solvent. The prerequisite results of this study would be further useful in synthesizing a hybrid biomaterial for tissue engineering.

Acknowledgment

The work was financially and technically supported by Tarbiat Modares University.

References

[1] D.W. Hutmacher, Scaffolds in tissue engineering bone and cartilage, Biomaterials, 21 (2000) 2529-2543.
[2] O. Tsigkou, I. Pomerantseva, J.A. Spencer, P.A. Redondo, A.R. Hart, E. O'Doherty, Y. Lin, C.C. Friedrich, L. Daheron, C.P. Lin, Engineered vascularized bone grafts, Proceedings of the National Academy of Sciences, 107 (2010) 3311-3316.
[3] L.G. Griffith, G. Naughton, Tissue engineering--current challenges and expanding opportunities, Science, 295 (2002) 1009-1014.
[4] L. Hench, J. Jones, Biomaterials, artificial organs and tissue engineering, Elsevier, 2005.
[5] J.R. Jones, L.M. Ehrenfried, L.L. Hench, Optimising bioactive glass scaffolds for bone tissue engineering, Biomaterials, 27 (2006) 964-973.
[6] J.R. Jones, G. Poologasundarampillai, R.C. Atwood, D. Bernard, P.D. Lee, Non-destructive quantitative 3D analysis for the optimisation of tissue scaffolds, Biomaterials, 28 (2007) 1404-1413.
[7] B.M. Novak, Hybrid nanocomposite materials—between inorganic glasses and organic polymers, Advanced Materials, 5 (1993) 422-433.
[8] E.M. Valliant, J.R. Jones, Softening bioactive glass for bone regeneration: sol–gel hybrid materials, Soft Matter, 7 (2011) 5083-5095.
[9] S. Labbaf, O. Tsigkou, K.H. Müller, M.M. Stevens, A.E. Porter, J.R. Jones, Spherical bioactive glass particles and their interaction with human mesenchymal stem cells *in vitro*, Biomaterials, 32 (2011) 1010-1018.
[10] O. Mahony, O. Tsigkou, C. Ionescu, C. Minelli, L. Ling, R. Hanly, M.E. Smith, M.M. Stevens, J.R. Jones, Silica-Gelatin Hybrids with Tailorable Degradation and Mechanical Properties for Tissue Regeneration, Advanced Functional Materials, 20 (2010) 3835-3845.
[11] J.R. Jones, Review of bioactive glass: from Hench to hybrids, Acta biomaterialia, 9 (2013) 4457-4486.
[12] R. Nagarale, V.K. Shahi, R. Rangarajan, Preparation of polyvinyl alcohol–silica hybrid heterogeneous anion-exchange membranes by sol–gel method and their characterization, Journal of membrane science, 248 (2005) 37-44.
[13] H.S. Mansur, H.S. Costa, Nanostructured poly (vinyl alcohol)/bioactive glass and poly (vinyl alcohol)/chitosan/bioactive glass hybrid scaffolds for biomedical applications, Chemical Engineering Journal, 137 (2008) 72-83.
[14] B. Lei, L. Wang, X. Chen, S.-K. Chae, Biomimetic and molecular level-based silicate bioactive glass–gelatin hybrid implants for loading-bearing bone fixation and repair, Journal of Materials Chemistry B, 1 (2013) 5153-5162.
[15] S. Trujillo, E. Pérez-Román, A. Kyritsis, J.L. Gómez Ribelles, C. Pandis, Organic–inorganic bonding in chitosan–silica hybrid networks: physical properties, Journal of Polymer Science Part B: Polymer Physics, 53 (2015) 1391-1400.
[16] G. Poologasundarampillai, C. Ionescu, O. Tsigkou, M. Murugesan, R.G. Hill, M.M. Stevens, J.V. Hanna, M.E. Smith, J.R. Jones, Synthesis of bioactive class II poly (γ-glutamic acid)/silica hybrids for bone regeneration, Journal of Materials Chemistry, 20 (2010) 8952-8961.
[17] Y. Ding, W. Li, T. Müller, D.W. Schubert, A.R. Boccaccini, Q. Yao, J.A. Roether, Electrospun Polyhydroxybutyrate/Poly (ε-caprolactone)/58S Sol–Gel Bioactive Glass Hybrid Scaffolds with Highly Improved Osteogenic Potential for Bone Tissue Engineering, ACS applied materials & interfaces, 8 (2016) 17098-17108.
[18] C. Brinker, Hydrolysis and condensation of silicates: effects on structure, Journal of non-crystalline solids, 100 (1988) 31-50.
[19] S. Lin, C. Ionescu, K.J. Pike, M.E. Smith, J.R. Jones, Nanostructure evolution and calcium distribution in sol–gel derived bioactive glass, Journal of Materials Chemistry, 19 (2009) 1276-1282.

[20] M.M. Pereira, J.R. Jones, L.L. Hench, Bioactive glass and hybrid scaffolds prepared by sol–gel method for bone tissue engineering, Advances in applied ceramics, (2013).
[21] E.M. Valliant, F. Romer, D. Wang, D.S. McPhail, M.E. Smith, J.V. Hanna, J.R. Jones, Bioactivity in silica/poly (γ-glutamic acid) sol–gel hybrids through calcium chelation, Acta biomaterialia, 9 (2013) 7662-7671.
[22] S. Pandey, S.B. Mishra, Sol–gel derived organic–inorganic hybrid materials: synthesis, characterizations and applications, Journal of sol-gel science and technology, 59 (2011) 73-94.
[23] N. Hüsing, U. Schubert, K. Misof, P. Fratzl, Formation and Structure of Porous Gel Networks from Si (OMe) 4 in the Presence of A (CH2) n Si (OR) 3 (A= Functional Group), Chemistry of Materials, 10 (1998) 3024-3032.
[24] M. Labieniec, C. Watala, PAMAM dendrimers—Diverse biomedical applications. Facts and unresolved questions, Central European Journal of Biology, 4 (2009) 434-451.
[25] G. Poologasundarampillai, B. Yu, O. Tsigkou, E. Valliant, S. Yue, P. Lee, R. Hamilton, M. Stevens, T. Kasuga, J. Jones, Bioactive silica–poly (γ-glutamic acid) hybrids for bone regeneration: effect of covalent coupling on dissolution and mechanical properties and fabrication of porous scaffolds, Soft Matter, 8 (2012) 4822-4832.
[26] D.A. Tomalia, H. Baker, J. Dewald, M. Hall, G. Kallos, S. Martin, J. Roeck, J. Ryder, P. Smith, Dendritic macromolecules: synthesis of starburst dendrimers, Macromolecules, 19 (1986) 2466-2468.
[27] L. Gabrielli, L. Russo, A. Poveda, J.R. Jones, F. Nicotra, J. Jiménez-Barbero, L. Cipolla, Epoxide opening versus silica condensation during sol–gel hybrid biomaterial synthesis, Chemistry–A European Journal, 19 (2013) 7856-7864.
[28] L. Gabrielli, L. Connell, L. Russo, J. Jiménez-Barbero, F. Nicotra, L. Cipolla, J.R. Jones, Exploring GPTMS reactivity against simple nucleophiles: chemistry beyond hybrid materials fabrication, RSC Advances, 4 (2014) 1841-1848.
[29] B.P. Mosher, C. Wu, T. Sun, T. Zeng, Particle-reinforced water-based organic–inorganic nanocomposite coatings for tailored applications, Journal of non-crystalline solids, 352 (2006) 3295-3301.
[30] S.-M. Shang, Z. Li, Y. Xing, J.H. Xin, X.-M. Tao, Preparation of durable hydrophobic cellulose fabric from water glass and mixed organosilanes, Applied Surface Science, 257 (2010) 1495-1499.
[31] Y.-L. Liu, Y.-H. Su, J.-Y. Lai, In situ crosslinking of chitosan and formation of chitosan–silica hybrid membranes with using γ-glycidoxypropyltrimethoxysilane as a crosslinking agent, Polymer, 45 (2004) 6831-6837.
[32] Y.-Y. Yu, W.-C. Chien, T.-W. Tsai, High transparent soluble polyimide/silica hybrid optical thin films, Polymer Testing, 29 (2010) 33-40.
[33] M.R. Knecht, D.W. Wright, Amine-terminated dendrimers as biomimetic templates for silica nanosphere formation, Langmuir, 20 (2004) 4728-4732.
[34] L. Russo, L. Gabrielli, E.M. Valliant, F. Nicotra, J. Jiménez-Barbero, L. Cipolla, J.R. Jones, Novel silica/bis (3-aminopropyl) polyethylene glycol inorganic/organic hybrids by sol–gel chemistry, Materials Chemistry and Physics, 140 (2013) 168-175.
[35] C. Acebo, X. Fernández-Francos, J.-I. Santos, M. Messori, X. Ramis, À. Serra, Hybrid epoxy networks from ethoxysilyl-modified hyperbranched poly (ethyleneimine) and inorganic reactive precursors, European Polymer Journal, 70 (2015) 18-27.
[36] Z. Zhuang, H. Yoshimura, M. Aizawa, Synthesis and ultrastructure of plate-like apatite single crystals as a model for tooth enamel, Materials Science and Engineering: C, 33 (2013) 2534-2540.
[37] F.A. Dourbash, P. Alizadeh, S. Nazari, A. Farasat, A highly bioactive poly (amido amine)/70S30C bioactive glass hybrid with photoluminescent and antimicrobial properties for bone regeneration, Materials Science and Engineering: C, 78 (2017) 1135-1146.